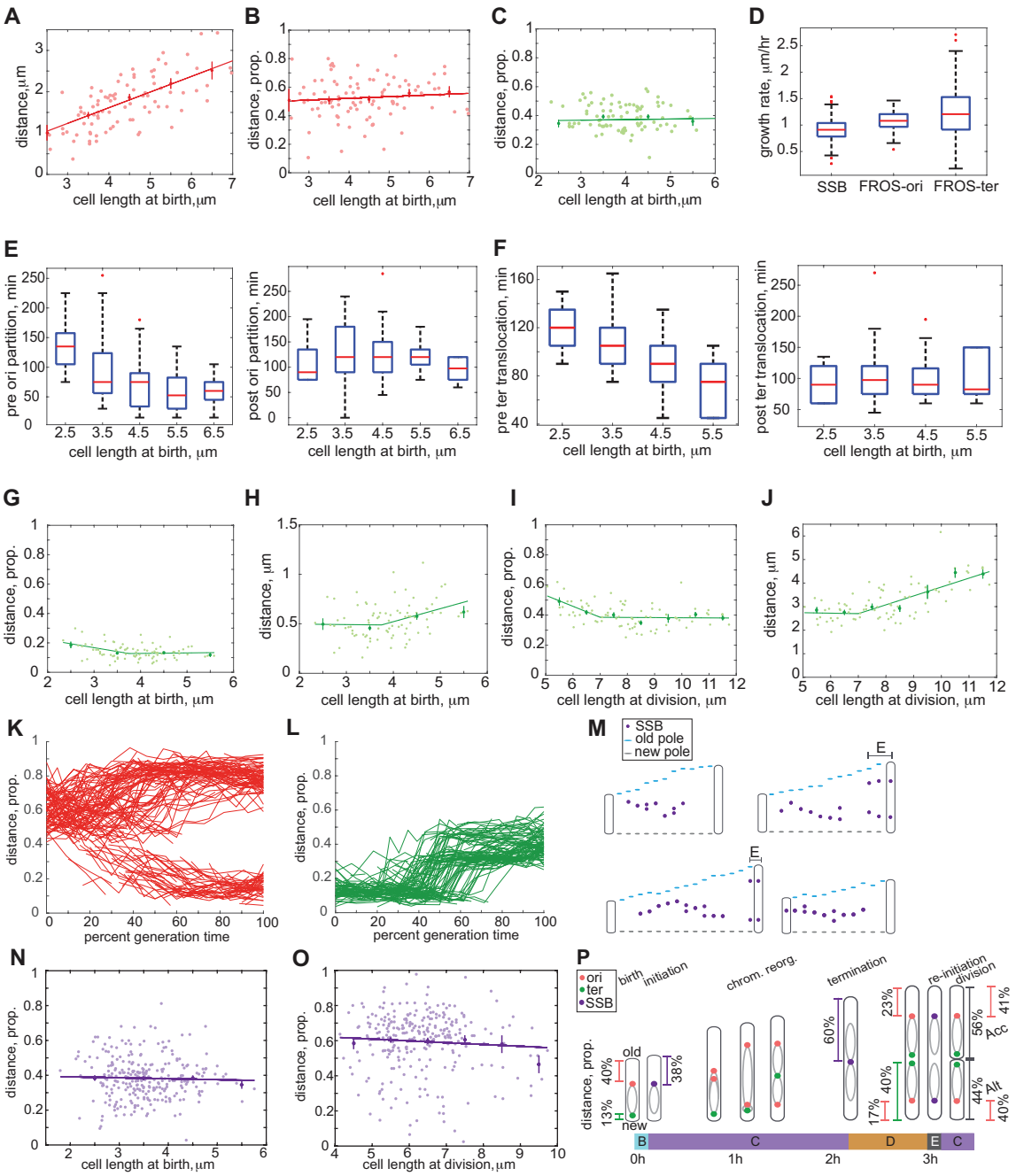

Figure S1. Timing and localization of chromosome replication and reorganization in *M. smegmatis.* Related to Figure 1. (A) Scatter plot of distance from the ori to the old cell pole at birth. The linear regression line shows a slope of 1.05 and Pearson correlation of r=0.66, p=3.86e-12. Red error bars display mean and SEM for cells binned by birth length. (**B-C)** Scatter plots of proportion of cell length from the ori (B) or ter (C) to the new cell pole one frame before partitioning (B) or one frame after translocation (C). Pearson correlation (B) r=0.10, p=0.35; Pearson correlation (C) r=-0.09, p=0.41 (**D)** Box plot of growth rates of reporter strains. Growth rates were calculated from cells growing in a microfluidics device during live imaging and were significantly different between all reporter strains. Wilcoxon rank sum tests show FROS Ori vs. FROS Ter p=0.02, FROS Ori vs. SSB p=7.16e-07, and FROS Ter vs. SSB p=3.45e-11. (**E-F)** Box plots of time before (left) and after (right) ori partitioning (E) and ter translocation (F). Box plots are binned by cell length at birth (bin ranges span 1 μm, centered as indicated on the axes). (**G)** Scatter plot of cell length at birth vs. the proportion of cell length from ter to new pole at birth with two-component line fit to measurements and green error bars displaying mean and SEM for cells binned by birth length. The position of ter is proportional to cell length at birth in cells born longer than 3.5 μm. (**H)** Scatter plot as in (F) of

cell length at birth vs. distance from ter to new pole at birth. Distance from the new pole to ter is constant in cells born shorter than 3.5 μm. **(I)** Scatter plot as in (F) of cell length at division vs. proportion of cell length from ter to new pole at division. Position of Ter is proportional to cell length at birth in cells longer than 7 μm at division. (**J)** Scatter plot as in (F) of cell length at division vs. distance from ter to new pole at division. Distance from the new pole to ter is constant in cells shorter than 7 μm at division. (**K)** Compilation of n=101 single cell line traces of FROS Ori localization plotted as percent interdivision time vs. proportion of cell length from the new pole. Non-continuous lines are caused when foci are out of focus or indiscernible for a frame and the data from that frame is omitted. (**L)** Single cell line traces (n=85) as in (K) of FROS Ter localization plotted as percent interdivision time vs. proportion of cell length from the new pole. **(M)** Representative single cell traces of SSB-GFP localization every 15 min for four individual cells, with and without E period. (**N-O)** Scatter plots of proportion of cell length from SSB to the old cell pole at initiation (B) or termination (C) versus cell length at birth (B) or division (C). The correlation line is fit to data and dark purple dots show mean with SEM bars for cells binned in 1 μm increments. Pearson correlation (B) r=-0.03, p=0.60; Pearson correlation (C) r=-0.06, p=0.28. (**P)** Model of *M. smegmatis* chromosome organization and replisome localization throughout the cell cycle as in 1J, depicted for cells that experience E period.

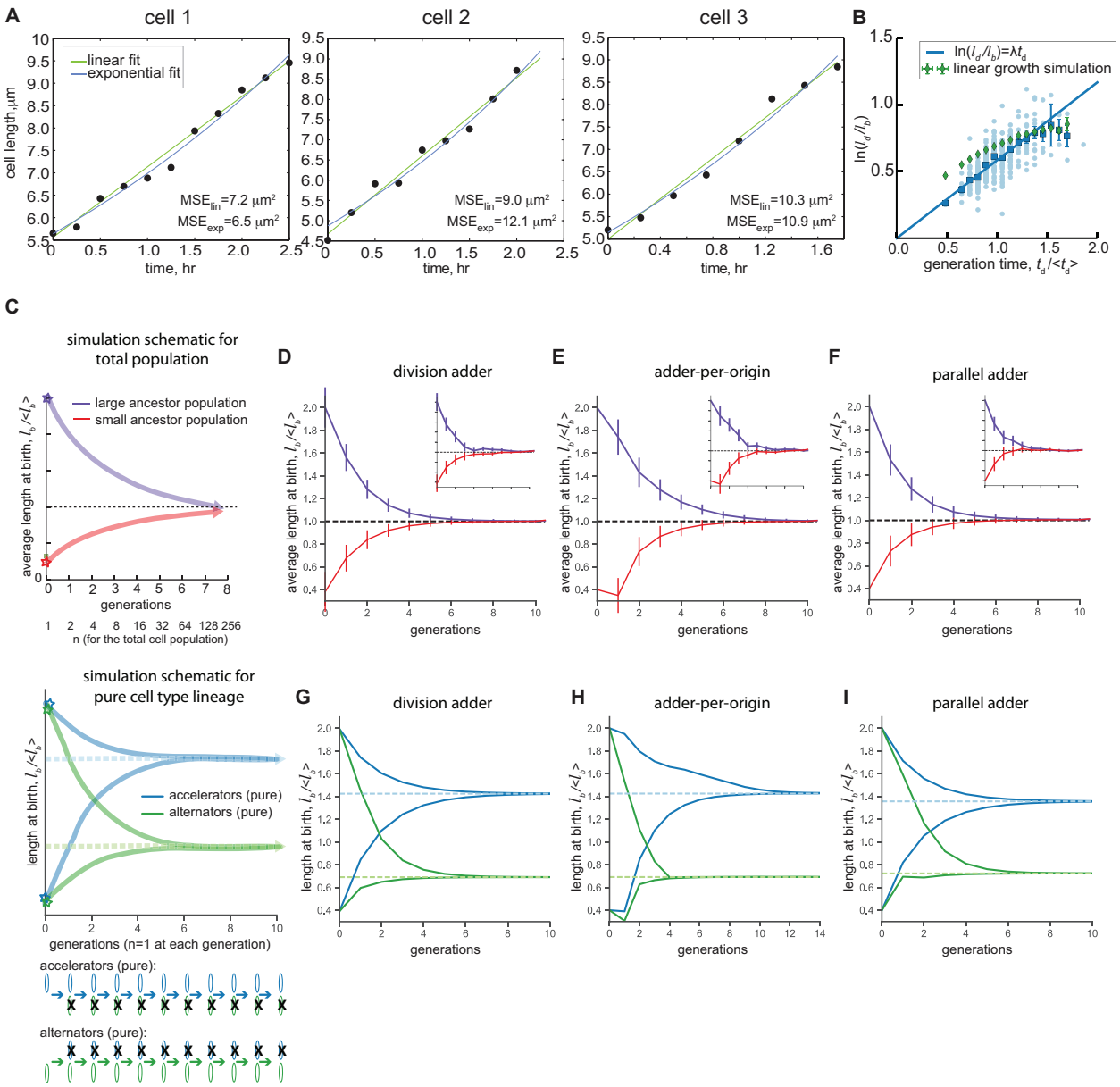

Figure S2. *M. smegmatis* growth mode and convergence of model simulations. Related to Figures 2 and 3. (A) Three representative single cell traces of *M. smegmatis* growth fit to linear and exponential growth models. The mean squared error (MSE) of both models fit to single cell growth data is similar, suggesting that growth data from imaging is insufficient to differentiate between linear and exponential growth models **(B)** Scatter plot of normalized generation time (t_d /< t_d >) vs. the natural log of division length/birth length ($\ln(l_d/l_b)$). <> is the population average of a measurement. Light blue dots are individual data points and blue squares are binned data with SEM bars. Data fit to $\ln(l_d/l_b) = \lambda t_d$ (blue line; λ = growth rate) are compared to simulation of linear growth (green diamonds). **(C)** Schematic of cell size convergence simulations corresponding with subfigures D-I. (Top) Schematic demonstrates convergence over several generations by following the average birth size of a multiplying cell population. Schematic shows progeny of hypothetical cells born extremely large (purple, an accelerator cell starting at the purple star) or small (red, an alternator cell starting at the red star). The number of cells in the total population of which the average is plotted is shown below the x-axis. (Bottom) Schematic of model simulation to demonstrate convergence over several generations of the pure accelerator cell lineage (blue) and pure alternator lineage (green) from individual large and small accelerator and alternator cells (e.g. four different simulations are shown as indicated with stars). For the accelerator lineage, the simulation begins with either a large or a small accelerator cell and then considers only

what happens with the accelerator daughter cell (alternator daughter cells are disregarded in this case, as diagramed below the x-axis). The birth length of the accelerator progenitor and its accelerator daughters is plotted for ten generations. Only one of the daughters is an accelerator so cell lengths are reported for only one cell per generation. The alternator progenitor cell and alternator daughters are similarly considered in the alternator lineage. Dashed light-colored lines plot the values of model predictions from the expressions given in section 6 of the Supplemental Experimental Procedures for each model. **(D-F)** Simulation of population cell size convergence to the predicted mean birth length without added noise and with added noise in growth rate, division ratio, and cell cycle timing (inset, see also Figure 3E) for the division adder (D), adder-per-origin (E), and parallel adder (F) models. The average cell birth length with SEM bars over ten generations is plotted for a hypothetical progenitor cell (accelerator) born 2.0x the population average and a hypothetical progenitor cell (alternator) born 0.4x the population average. See (C, top) for a schematic description and legend. Parameters are the same as those used to generate Figure 3E in the main text. (**G-I**) Simulation of pure accelerator and alternator lineages to demonstrate convergence of the longest and shortest cell subpopulations in the division adder (G), adder-per-origin (H), and parallel adder (I) models. See (C, bottom) for a schematic description and legend.

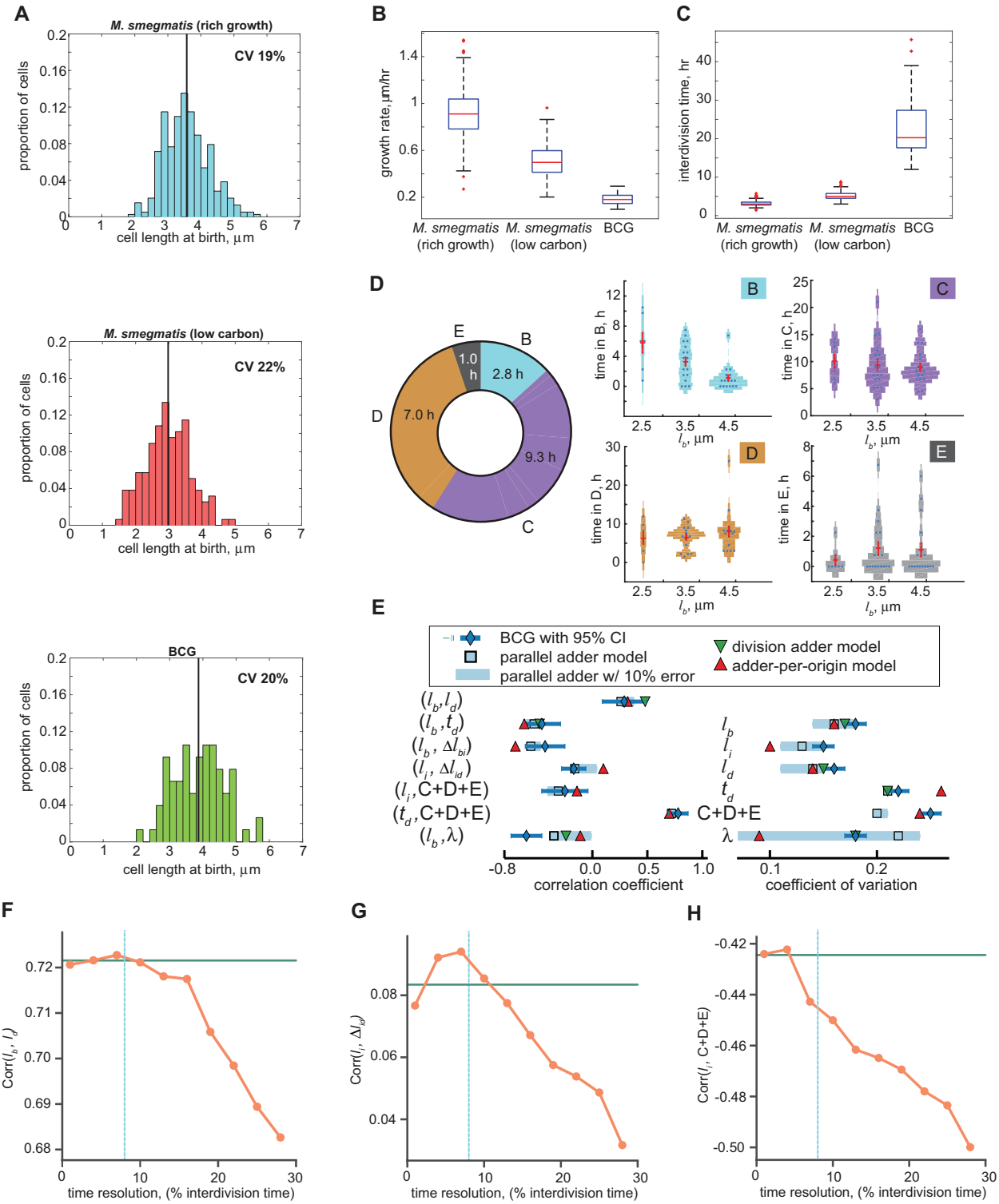

Figure S3. Mycobacterial growth and division in fast and slow growth conditions. Related to Figure 4. (A) Histograms of cell birth lengths of *M. smegmatis* growing in rich medium (7H9), carbon limited medium, and BCG in rich medium. Mean birth length in each condition is displayed as a black line. **(B)** Box plots of *M. smegmatis* growth rate in rich medium (7H9), carbon limited medium, and BCG in rich medium **(C)** Box plots of *M. smegmatis* interdivision times in rich medium (7H9), carbon limited medium, and BCG in rich medium **(D)** BCG cell cycle timing, as in Figure 2E **(E)** Chart of BCG cell cycle correlation coefficients and coefficients of variation showing BCG measurements normalized to population mean compared to model simulation, as in Figure 3B. **(F)** Line graph

comparing the correlation coefficient of birth length vs. division length (l_b, l_d) from simulations in which data are collected at limited time resolution. Orange circles plot numerically obtained correlation coefficients as a function of the time resolution in percentage interdivision time. The green line plots the correlation coefficient without limited time resolution. Blue dotted line marks the time resolution from *M. smegmatis* experiments in rich medium (7H9). (**G**). Line graph (as in Figure S3E) displaying the simulated correlation coefficient of length at initiation vs. growth from initiation to division (l_i, Δl_{id}) as a function of the time resolution. Blue dotted line marks the time resolution from *M. smegmatis* experiments in rich medium (7H9). (**H**). Line graph (as in Figure S3E) displaying the simulated correlation coefficient of length at initiation vs. time from initiation to division (l_i, C+D+E) as a function of the time resolution. Blue dotted line marks the time resolution from *M. smegmatis* experiments in rich medium (7H9).

Models relate cell size control and cell cycle progression in one of three ways – time, size, or growth.
- Time increments measure minutes between events, e.g. cells grow 100 min. before division
- Size measures the absolute length at an event, e.g. cells divide once reaching 7 μm in length
- Growth increments measure change in length between two events, e.g. cells divide after adding 4 μm to original length

Models presented in this paper utilize growth increments (division adder), a combination of growth and time increments (adder-per-origin), or multiple growth increments (sequential adder, parallel adder) to describe coordination of cell cycle events with each other.

models	testing
division adder constant Δl_{bd} 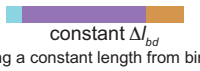 constant Δl_{bd}  Cells divide after growing a constant length from birth: $l_d^z = l_b + \Delta l_{bd}^z$. The division adder is also called "adder" and "incremental model" elsewhere. • Cell size at birth converges to the length increment ($< l_b > = \Delta l_{bd}$). • Does not consider DNA replication timing.	**Growth increment:** growth between divisions independent of birth length (Δl_{bd} not correlated with l_b). Consistent with *M. smegmatis* in rich medium but not low carbon medium or BCG (Figs. 2B, 4B, SX). **Division timing:** inverse log relationship between birth size and time to division ($t_d = \frac{1}{\lambda}\ln(1+\Delta l_{bd}/l_b)$). Inconsistent with *M. smegmatis* in rich medium (Fig. 2C). **Correlations and CVs:** determined by simulations. Many values inconsistent with data (Figs. 3B, 4B, S3E).
adder-per-origin constant Δl_{ii} 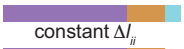 constant Δl_{ii} 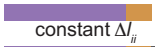 constant C+D (time) 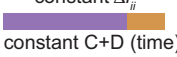 constant C+D+E (time)  An adder mechanism is implemented at initiation. Division and initiation of DNA replication is coordinated by two controls: 1) Division occurs at a constant time after initiation (Cooper-Helmstetter model): $l_d = l_i e^{\lambda(C+D)}$ 2) Initiation occurs after a constant growth increment (per origin) after previous initiation: $(l_i)^{total} = l_i^z + O\Delta l_{ii}^z$ • Initiation and division depend on prior initiation and number of origins (O) and accounts for cells that begin next round of replication before division (e.g. E period) • Cell size at birth converges to $< l_b > = \Delta l_{ii}^z e^{\lambda(C+D)}$	**Division timing:** constant time between initiation and division, independent of size ($\Delta t_{id} = C+D+E$ not correlated with l_i). Inconsistent with *M. smegmatis* growth in rich medium (Fig. 2F). **Correlations and CVs:** determined by simulations. Many values inconsistent with data (Figs. 3B, 4B, S3E).
sequential adder constant Δl_{id} 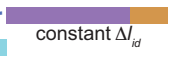 constant Δl_{id}  constant Δl_{bi}  constant Δl_{bi}  ~~constant Δl_{bi}~~ Similar to division adder, except constant volume increment is separated into two components: 1) Cells initiate DNA replication after a constant growth increment since birth. 2) Cells divide after a constant growth increment from initiation. • Cell size at birth converges as described in the division adder • Because new initiation begins before division in cells with an E period, we cannot fully diagram this model (red X and line through)	**Growth increment:** Growth birth to initiation and initiation to division independent of birth length (Δl_{bi} and Δl_{id} not correlate d with l_b). Existence of initiation of a second round of DNA replication before division (E period) excludes this model.
parallel adder constant Δl_{ii} 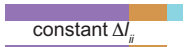 constant Δl_{ii}  constant Δl_{id} 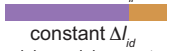 constant Δl_{id} 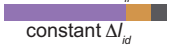 Similar to the adder-per-origin model, except constant time initiation to division is replaced by a constant growth increment from initiation to division, Δl_{id} 1) Cells initiate DNA replication after growing a constant volume (per origin) since the last initiation event, $(l_i)^{total} = l_i^z + O\Delta l_{ii}^z$ 2) Cells divide after growing a constant volume (per origin) since initiation, $(l_d^z = l_i^z + O\Delta l_{id}^z)$ • Initiation and division depend on prior initiation and number of origins (O) and accounts for cells that begin next round of replication before division (e.g. E period; Fig. 3A) • Cell size at birth converges to the average of the length increments Δl_{ii} and Δl_{id}.	**Growth increment:** growth initiation to division independent of birth length (Δl_{id} is not correlated with l_i). This is consistent with our data -(Figs. 2G, 2B, 4B, S3E). **Correlations and CVs**: determined by model simulations. These values are consistent with data (Figs. 3B, 4B, S3E).

Figure S4. Information box summary of cell size control models. Related to Figures 2 and 3.
All models are based on exponential growth and account for differences in size and growth rate of accelerator vs. alternator cells (Figure S2A & Supplemental Experimental Procedures section 5). The models and derivations of model properties are described fully in Supplemental Experimental Procedures section 6. The abbreviations are as follows: l is cell length; t is time; subscripts b, d, and i indicate birth, division, and initiation of DNA replication, respectively; z designates either the accelerator or alternator subpopulations; and λ is the exponential growth constant. Open circles represent number of origins (O) present in different phases of the cell cycle. Growth between two events is represented by Δ, with subscripts noting the starting and ending event.

CVs	v-snapping/ pinching division	FM division	Parallel adder	Adder-per-origin	Division adder
l_b	0.19	0.22	0.19	0.22	0.21
l_i	0.18	0.20	0.18	0.17	-
l_d	0.17	0.17	0.15	0.17	0.16
t_d	0.20	0.20	0.21	0.25	0.26
C+D+E	0.22	0.22	0.20	0.21	-
λ	0.18	0.18	0.19	0.17	0.27

Correlations	v-snapping/ pinching division	FM division	Parallel adder	Adder-per-origin	Division adder
l_b, l_d	0.65±0.06	0.78±0.08	0.66	0.56	0.63
l_b, t_d	-0.32±0.09	-0.32±0.15	-0.43	-0.56	-0.41
v_b, v_i-v_b	-0.19±0.10	-0.29±0.15	-0.32	-0.47	-
l_i, l_d-l_i	0.05±0.10	0.12±0.17	0.00	0.18	-
l_i, C+D+E	-0.35±0.09	-0.14±0.16	-0.41	-0.26	-
t_d, C+D+E	0.79±0.04	0.78±0.08	0.81	0.70	-
l_b, λ	-0.39±0.09	-0.41±0.14	-0.24	-0.18	-0.22

Table S1. Measured and simulated CVs and correlations. Related to Figure 3. Cell cycle parameter CVs (top) and correlations (bottom) were measured from v-snapping/pinching dividing cells (n=380) and FM dividing cells (n=129) and compared to cell size control model simulations from the parallel adder model, adder-per-origin model, and division adder model. Correlation measurements are displayed with ± 95% confidence intervals. Variables represented are l_b = birth length, l_d = length before division, l_i = length at initiation of DNA replication, t_d = interdivision time, Δl = length increment between the b=birth, i=initiation, and d=division events indicated in the subscripts, C+D+E = total time spent in these periods, and λ = growth rate. All measurements were normalized to the population mean.